RSC Advances

COMMUNICATION

View Article Online
View Journal | View Issue

Cite this: *RSC Adv.*, 2016, **6**, 115298

Received 24th August 2016
Accepted 26th November 2016

DOI: 10.1039/c6ra21260c

www.rsc.org/advances

Carbazole-based two-photon fluorescent probe for selective imaging of mitochondrial hydrogen peroxide in living cells and tissues†

Kai Zhang,‡[bd] Wei Wu,‡[a] Yinhui Li,*[ab] Mingtai Sun,[c] Huan Yu*[c] and Man Shing Wong*[b]

This paper reported a two-photon fluorescent probe for mitochondrial H_2O_2 detection and imaging based on the incorporation of a sensing boronate ester and an organelle-targeting triphenylphosphonium moiety onto the carbazole fluorophore. The probe exhibits a fast "turn on" response, good selectivity toward H_2O_2 and high specificity for mitochondria.

As a typical ROS, hydrogen peroxide (H_2O_2) can mediate diverse physiological responses and serve as the second messenger in normal cellular signal transduction.[1] In mammalian cells, mitochondria have been demonstrated as main venues for the production of H_2O_2 and the generated H_2O_2 can participate in redox signaling through reversible oxidation of cysteine residues in target proteins.[2] Excessive production of H_2O_2 in mitochondria will induce oxidative damage and cause physiological changes and diseases, such as cancer, cardiovascular disorders, and Alzheimer's disease.[3] Therefore, specific, localizable and readily deployable tools for reliable and precise intracellular measurement of H_2O_2 are imperative. Up to now, a variety of analytical means, such as spectrophotometry, electrochemistry, and MRI[4] together with recognition principles have been used to develop effective hydrogen peroxide sensors. The fluorescence assay for H_2O_2 detection in human physiology and pathology, which employs H_2O_2-triggered oxidative cleavage of boronate to phenol, sulfonate group hydrolysis,[5] triphenylphosphine oxidation,[6] Baeyer–Villiger type reaction[7] and metal complex mediated reaction,[8] has shown an extensive prospect because of the high sensitivity and specificity as well as capability of real-time and *in situ* imaging analysis. Although fluorescent probes were well competent to image the spatial and temporal distribution of cellular H_2O_2, how to maintain the cell viability following prolonged exposure to excitation illumination was still a challenge.

Two-photon microscopy (TPM) can record the most subtle internal structure deep into tissue with low cell damage by using two near-infrared photons for the excitation, which provides greater tissue penetration depth and higher spatial resolution.[9] A variety of TP probes equipped with an organelle-targeting moiety such as tertiary amine, pyridinium or triphenyl-phosphonium group for labeling lysosomes and mitochondria have been developed which provided organelle-specific imaging with good spatial and temporal resolution. The superior tracing and imaging functions of TPM can be used for determining the spatial and temporal dynamics of reactive oxygen metabolites in a living system, especially for elucidating the diverse roles of H_2O_2 in a complex biological environment. It is particularly beneficial to use TPM for reactive oxygen species (ROS) and reactive nitrogen species (RNS) detections in a complex biological system. Some TP fluorescent probes have been shown to image hypochlorous acid,[10] superoxide anion[11] and nitric oxide[12] in cellular environment. Up to date, there are only a handful of TP probes designed for intracellular H_2O_2 imaging,[13] especially for mitochondrial or lysosomal H_2O_2.[14] Because of the rapid metabolic process and constantly changed concentration of intracellular H_2O_2, there is a great demand for developing TPM probes to monitor the H_2O_2 production and consumption in mitochondria with fast response time and low detection limit to better understand the cellular and physiological roles of mitochondrial H_2O_2.

In this work, a TP fluorescent probe CBZ-H_2O_2 was synthesized by incorporating a boronate functionality as a H_2O_2 recognition site and the triphenylphosphonium group as mitochondrial targeting moiety into the fluorescent carbazole framework. The presence of boronic ester group at the 3-

[a]*College of Chemistry, Xiangtan University, Xiangtan, 411105, People's Republic of China. E-mail: yinhuili16@163.com*

[b]*Department of Chemistry, Hong Kong Baptist University, Kowloon Tong, Hong Kong, People's Republic of China. E-mail: mswong@hkbu.edu.hk*

[c]*Institute of Intelligent Machines, Chinese Academy of Sciences, Hefei, Anhui 230031, People's Republic of China. E-mail: hyu@iim.ac.cn*

[d]*College of Preclinical Medicine, Southwest Medical University, Luzhou, 646000, People's Republic of China*

† Electronic supplementary information (ESI) available. See DOI: 10.1039/c6ra21260c

‡ These author contributed equally to this work.

position of a carbazole scaffold would quench the TP fluorescence of CBZ-H_2O_2. After treatment with H_2O_2, a highly fluorescent product would be subsequently yielded due to the chemospecific deprotection of boronate to hydroxyl functionality. Compared with the existing TP probes for mitochondrial H_2O_2, CBZ-H_2O_2 exhibited a fast response time (~15 min), improved sensitivity and low interference from other ROS. Importantly, it can be applied for direct imaging of mitochondrial H_2O_2 in living cells and frozen slice of rat liver with satisfactory imaging results.

The TP probe, CBZ-H_2O_2 was developed for localized detection of H_2O_2 concentration variations in mitochondrial. The synthetic routes and recognition principle were shown in Schemes 1 and 2, respectively. The molecular structure of CBZ-H_2O_2 was fully characterized with ^{1}H NMR and ^{13}C NMR as well as ^{31}P NMR (Fig. S1–S4 in the ESI†). We then investigated the absorption and fluorescence properties of CBZ-H_2O_2 in PBS/DMSO (4/1 v/v, 20 mM, pH 7.4) solution at room temperature. As shown in Fig. S5,† the maximum absorbance at 340 nm of CBZ-H_2O_2 was gradually shifted to 360 nm after adding H_2O_2, with slightly enhanced absorbance. The same trend was followed for the maximum fluorescence intensity at 396 nm. In the presence of H_2O_2, the emission band exhibited an apparent 35 nm red shift and the fluorescence intensity dramatically increased nearly four times. The sensitive spectral response confirmed the specific reaction between CBZ-H_2O_2 and H_2O_2.

In order to optimize the pH value for the best response, we then investigated the fluorescence response of CBZ-H_2O_2 toward H_2O_2 in buffer solution at different pH ranging from 4.0 to 10.0. The intensity of CBZ-H_2O_2 remained consistent at different pH values. Upon treatment with H_2O_2, compared with the acidic region, the fluorescence intensity displayed a more noticeable enhancement in the alkaline region between 7.0 and 10.0 as shown in Fig. S6.† Therefore, it is advantageous to carry out the experiments in the buffer solution with pH value of 7.4, which is promising for biological applications.

Fluorescence titration of H_2O_2 was conducted using 1.0 μM of CBZ-H_2O_2 and different concentration of H_2O_2 in PBS (20 mM, pH 7.4) containing 20% DMSO. As shown in Fig. 1A, the fluorescence response of probe was highly sensitive to the amount of H_2O_2. When the concentration of H_2O_2 went to 80 μM, the fluorescence enhancement reached a plateau, and further increase in the concentration would not boost the signal. Moreover, the dose-dependent fluorescence enhancement showed a good linearity between the F/F_0 and the concentrations of H_2O_2 in a wide range from 0 to 30 μM with a detection limit (3σ/slope) of 1.96 μM (Fig. 1B, inset), where F_0 and F corresponded to the fluorescence intensities at 430 nm of CBZ-H_2O_2 before and after adding H_2O_2, respectively. Compared with the reported fluorescent probes for H_2O_2, CBZ-H_2O_2 presents an improved detection sensitivity, which exhibited the potential to be used in monitoring physiological concentration of mitochondrial H_2O_2.

The real-time kinetic response of CBZ-H_2O_2 toward H_2O_2 was measured by recording the fluorescence emission as a function of time. As shown in Fig. 1C, in the first three minutes, the fluorescence intensity of CBZ-H_2O_2 remained steady and constant under irradiation. Upon the addition of H_2O_2, a drastic

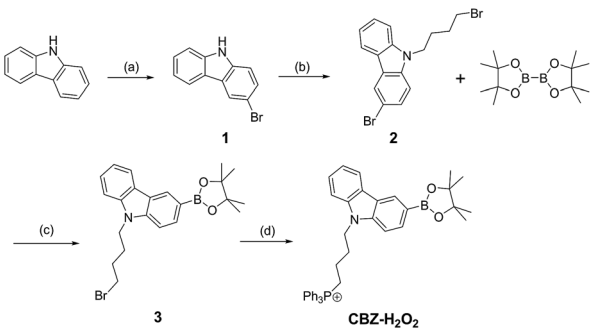

Scheme 1 Synthesis of probe CBZ-H_2O_2. Reagents and conditions: (a) NBS, DMF, 88%; (b) NaOH, 1,4-dibromobutane, toluene/H_2O, 86%; (c) Pd(dppf)Cl_2, dioxane, 50%; (d) triphenylphosphine, acetonitrile, 90%.

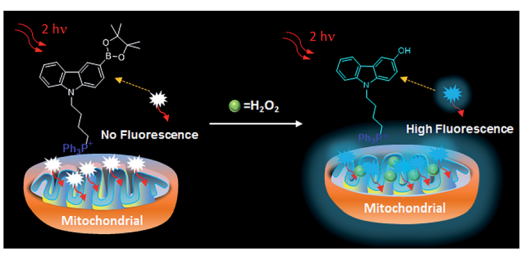

Scheme 2 The recognition mechanism of CBZ-H_2O_2 to H_2O_2 in mitochondria.

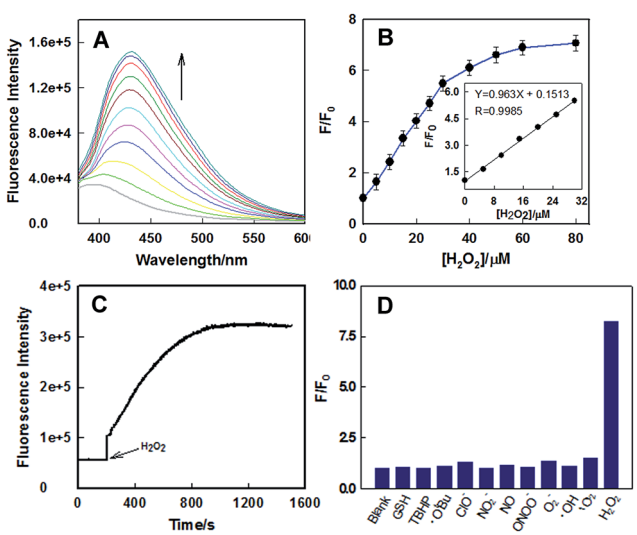

Fig. 1 (A) Fluorescence emission spectra of CBZ-H_2O_2 (1.0 μM) in the presence of different concentrations of H_2O_2 (0–80 μM) in PBS (20 mM, pH 7.4) containing 20% DMSO. (B) Calibration curve of CBZ-H_2O_2 as a function of H_2O_2 concentrations. The curve was plotted with the fluorescence intensity *vs.* H_2O_2 concentration after incubation for 15 min. (C) Real-time fluorescence intensity records of CBZ-H_2O_2 (1.0 μM) upon addition of H_2O_2 (50 μM) in PBS (20 mM, pH 7.4). $\lambda_{ex}/\lambda_{em}$ = 350 nm/430 nm. (D) Fluorescence responses of 1.0 μM CBZ-H_2O_2 to various reactive oxygen species ($O_2^{\bullet-}$, HO$^\bullet$, ClO^-, $^1O_2$), reactive nitrogen species (NO, NO_2^-, $ONOO^-$), TBHP, O^{t}Bu, and GSH.

fluorescence enhancement was observed and the intensity reached plateaus within 15 minutes, indicating that the reaction proceeded faster than a majority of reported H_2O_2 probes. Considering that ROS and RNS are involved in a wide range of physiological and pathological processes, the selectivity of CBZ-H_2O_2 over ROS, RNS and other potentially competing species was investigated. Treatment of CBZ-H_2O_2 with other ROS ($O_2^{\bullet-}$, $HO^{\bullet}$, ClO^-, $^1O_2$), RNS (NO, NO_2^-, $ONOO^-$), TBHP, O^{t}Bu, and GSH afforded negligible effects on the fluorescence intensity of CBZ-H_2O_2 as shown in Fig. 1D. Only the presence of H_2O_2 could induce dramatically intensity enhancement, suggesting that CBZ-H_2O_2 exhibited a good selectivity toward H_2O_2 in complex physiological conditions.

To investigate the reaction mechanism of CBZ-H_2O_2 with H_2O_2, the differences of ^{1}H NMR spectra of CBZ-H_2O_2 and the corresponding H_2O_2-reaction product were carefully analyzed and compared as shown in Fig. S7.† Upon the addition of H_2O_2, the resonance signal of CBZ-H_2O_2 at 8.44 ppm gradually moved to the high field, while a new and distinct resonance signal appeared and increased in intensity at 9.04 ppm over a period of 30 min. These changes of NMR signals corresponded to the phenolic proton of the reaction product, supporting the transformation of carbazole boronate to its corresponding phenol in the presence of H_2O_2.

With a good understanding of the sensitivity and selectivity of spectroscopic responses of the CBZ-H_2O_2 probe for detecting H_2O_2 *in vitro*, we sought to apply it for the detection of H_2O_2 in living cells. Before carrying out the cell imaging experiments, the cytotoxicity of CBZ-H_2O_2 with concentrations from 0 to 20 μM and its reaction product with H_2O_2 were determined using MTT viability assay. As shown in Fig. S8,† CBZ-H_2O_2, and its reaction product with H_2O_2 showed low toxicity to HeLa cells, with relatively high cell viability greater than 85% after incubation for 24 h. The results suggested that CBZ-H_2O_2 probe showed superior biocompatibility for cell imaging. To further investigate the application of CBZ-H_2O_2 in bio-imaging, the TP action cross-section ($\Phi\delta_{max}$) was determined from the two-photon excited fluorescence (TPEF) spectra of CBZ-H_2O_2 in the absence and presence of H_2O_2 by using rhodamine-6G in methanol as the reference, as shown in Fig. S9,† the $\Phi\delta_{max}$ of CBZ-H_2O_2 is 4.8 GM at 720 nm, but $\Phi\delta_{max}$ increased to 65 GM after addition of H_2O_2. Such a drastic enhancement in TPEF indicates that CBZ-H_2O_2 is a potential two-photon probe for imaging H_2O_2 in living specimens.

To investigate the mitochondria-targeting function of CBZ-H_2O_2 and its application as a TP probe for detecting H_2O_2 level changes in mitochondria, a co-localization experiment was carried out to confirm mitochondria-localization specificity of CBZ-H_2O_2 in HeLa cells by co-staining it with Mito Tracker red (1.0 μM), a commercially available mitochondria tracker. As shown in Fig. 2, the red fluorescent from Mito Tracker (2c, red channel, λ_{ex} = 590 nm; λ_{em} = 620–660 nm) and the blue fluorescent from CBZ-H_2O_2 in H_2O_2 solution (2b, blue channel, λ_{ex} = 720 nm; λ_{em} = 420–460 nm) overlapped very well, and the Pearson's co localization coefficient was calculated at 0.925. The results indicated that CBZ-H_2O_2 was distributed mainly in the mitochondria with mitochondria-positioning capability.

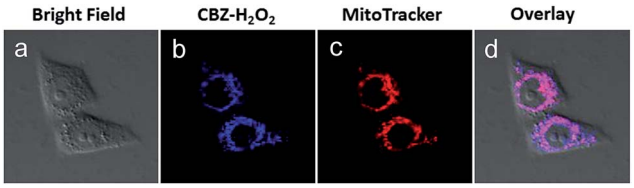

Fig. 2 Localization of CBZ-H_2O_2 in the mitochondrial of HeLa cells. Cells were stained with (a) bright field, (b) 10.0 μM CBZ-H_2O_2 with H_2O_2 solution (50.0 μM) for 30 min at 37 °C (λ_{ex} = 720 nm, λ_{em} = 420–460 nm). (c) 1.0 μM Mito Tracker red (λ_{ex} = 590 nm, λ_{em} = 620–660 nm). (d) Overlay of images (b) and (c).

To demonstrate the potential bio-applications of CBZ-H_2O_2, the ability of probe to track endogenous burst of H_2O_2 produced within HeLa cells was evaluated. Firstly, CBZ-H_2O_2 was incubated with live HeLa cells for 30 min to guarantee completely entry in cells. As shown in Fig. 3, two-photon confocal fluorescence images taken at an excitation of 720 nm for HeLa cells incubated with 10.0 μM CBZ-H_2O_2 indicated that the probe was cell-permeable. When HeLa cells were stained with CBZ-H_2O_2 only, the image displayed extremely weak fluorescence induced by the intrinsic H_2O_2 produced by cell metabolism. Further more, the endogenous H_2O_2 was produced by stimulating HeLa cells with phorbol myristate acetate (PMA), which induced a phagocytosis-associated H_2O_2 generation.[15] And remarkable fluorescence enhancement from the cells was observed when the cells was stimulated with PMA (1.0 μg mL^{-1}) before introducing CBZ-H_2O_2. It is evident that the obvious signal enhancement is mainly due to the reaction between CBZ-H_2O_2 and endogenous H_2O_2. In order to further validate the main functions of H_2O_2 for signal increases, HeLa cells were then treated with DMSO (0.5%) as a ROS scavenger before loading CBZ-H_2O_2 for 30 min.[16] The presence of CBZ-H_2O_2 in cells did not show any fluorescence response due to the clearance of intracellular H_2O_2.

Encouraged by the success of cell imaging with CBZ-H_2O_2 for mitochondrial H_2O_2, we further investigated whether it could be used for H_2O_2 imaging in deep-tissue. The images were

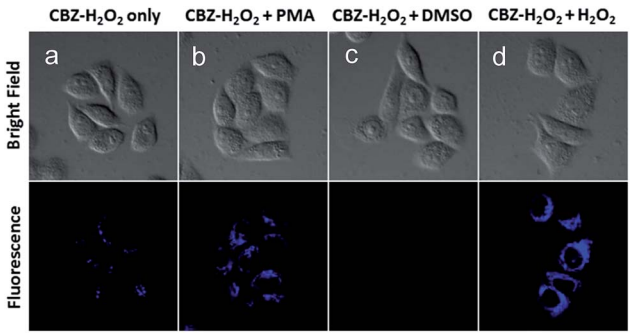

Fig. 3 Fluorescence images of HeLa cells using CBZ-H_2O_2 under different conditions. (a) Cells incubated with CBZ-H_2O_2 only; (b) cells pretreated with PMA (1.0 μg mL^{-1}) and then loading CBZ-H_2O_2 for 30 min; (c) cells followed treated with DMSO (0.5%) and then loading CBZ-H_2O_2 for 30 min; (d) cells incubated with CBZ-H_2O_2 and adscititous H_2O_2.

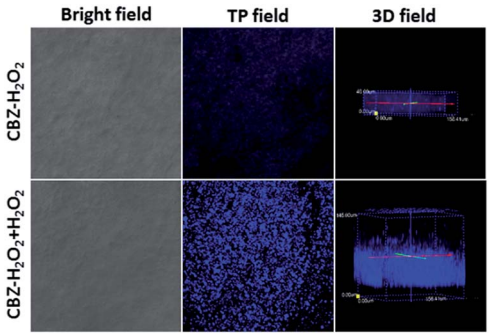

Fig. 4 TP confocal microscopy bright-field images (left) and fluorescence images (middle) of rat liver frozen slice after incubation with CBZ-H_2O_2 and CBZ-H_2O_2 + H_2O_2, respectively. And 3D TP confocal fluorescence images (right) of CBZ-H_2O_2 and CBZ-H_2O_2 + H_2O_2 accumulated along the *z* direction at a depth of 0–40 μm and 0–105 μm with 40× magnification, respectively.

obtained from 1.0 mm-thick rat liver frozen slice which was treated with CBZ-H_2O_2 before and after incubating with 50 μM H_2O_2 at 37 °C. As shown in Fig. 4, the slice treated with CBZ-H_2O_2 only exhibited feeble fluorescence signal, whereas the addition of H_2O_2 to the slice distinctly intensified the fluorescence signal, clearly demonstrating the capability of CBZ-H_2O_2 for H_2O_2 detection in tissue. Subsequently, to further investigate the utility for deep tissue imaging, the 3D two-photon confocal fluorescence imaging along the *z*-direction were taken by treating the slice with CBZ-H_2O_2 in the absence and presence of H_2O_2. The Z-scanning confocal imaging showed that luminescence emission of CBZ-H_2O_2 present in the penetration depth of 40 μm, while the presence of H_2O_2 in tissue made the emission deeper to 105 μm, indicating that CBZ-H_2O_2 has excellent capacity of monitoring H_2O_2 at a greater depth of tissue using two-photon microscopy.

Conclusions

In summary, we have designed and synthesized a new two-photon fluorescent "turn-on" probe for mitochondrial H_2O_2 detection. The probe consists of a boronate ester functionality as a sensing site, a carbazole derivative as a fluorophore and a triphenylphosphonium moiety as a mitochondrial-targeting localizer. It exhibits not only fast response and high selectivity over other ROS, RNS and related biomolecules but also low detection limit of 1.96 μM. Co-localization experiments clearly demonstrated that CBZ-H_2O_2 selectively localizes to and accumulates in the mitochondria. CBZ-H_2O_2 is also sensitive to both exogenous and endogenous H_2O_2. By using two-photon fluorescence microscopy, it can detect H_2O_2 in living cells and tissues at a depth of 105 μm for a long period of time with excellent imaging quality. This probe will allow in-depth investigation of the roles and functions of H_2O_2 in complex biological systems.

Acknowledgements

This work was supported by the National Natural Science Foundation of China (21305036, 21507135), Hunan Provincial Natural Science Foundation of China (2015JJ3035), China Postdoctoral Science Foundation funded project (2015M580685) and Anhui Province Natural Science Foundation of China (1608085MB30).

Notes and references

1 B. Halliwell and J. M. C. Gutteridge, *Free Radicals in Biology and Medicine*, Clarendon Press, Oxford, UK, 3rd edn, 1999.
2 L. J. Chen, R. Na, M. J. Gu, A. B. Salmon, Y. H. Liu, H. Y. Liang, W. B. Qi, H. V. Remmen, A. Richardson and Q. T. Ran, *Aging Cell*, 2008, **7**, 866.
3 (*a*) H. K. Seitz and F. Stickel, *Nat. Rev. Cancer*, 2007, **7**, 599; (*b*) H. Ohshima, M. Tatemichi and T. Sawa, *Arch. Biochem. Biophys.*, 2003, **417**, 3; (*c*) A. M. Shah and K. M. Channon, *Heart*, 2004, **90**, 486; (*d*) M. T. Lin and M. F. Beal, *Nature*, 2006, **443**, 787.
4 (*a*) S. L. Hempel, G. R. Buettner, Y. Q. O'Malley, D. A. Wessels and D. M. Flaherty, *Free Radical Biol. Med.*, 1999, **27**, 146; (*b*) M. Y. Hua, H. C. Chen, R. Y. Tsai, Y. L. Leu, Y. C. Liu and J. T. Laie, *J. Mater. Chem.*, 2011, **21**, 7254.
5 (*a*) A. R. Lippert, K. Y. Keshari, J. Kurhanewicz and C. J. Chang, *J. Am. Chem. Soc.*, 2011, **133**, 3776; (*b*) G. C. Van de Bittner, C. R. Bertozz and C. J. Chang, *J. Am. Chem. Soc.*, 2013, **135**, 1783; (*c*) M. C. Chang, A. Pralle, E. Y. Isacoff and C. J. Chang, *J. Am. Chem. Soc.*, 2004, **126**, 15392; (*d*) B. C. Dickinson, C. Huynh and C. J. Chang, *J. Am. Chem. Soc.*, 2010, **132**, 5906; (*e*) E. W. Miller, A. E. Albers, A. Pralle, E. Y. Isacoff and C. J. Chang, *J. Am. Chem. Soc.*, 2005, **127**, 16652; (*f*) H. Maeda, Y. Fukuyasu, S. Yoshida, M. Fukuda, K. Saeki, H. Matsuno, Y. Yamauchi, K. Yoshida, K. Hirata and K. Miyamoto, *Angew. Chem., Int. Ed.*, 2004, **43**, 2389; (*g*) K. Xu, B. Tang, H. Huang, G. Yang, Z. Chen, P. Li and L. An, *Chem. Commun.*, 2005, **48**, 5974.
6 N. Soh, O. Sakawaki, K. Makihara, Y. Odo, T. Fukaminato, T. Kawai, M. Irie and T. Imato, *Bioorg. Med. Chem.*, 2005, **13**, 1131.
7 M. Abo, Y. Urano, K. Hanaoka, T. Terai, T. Komatsu and T. Nagano, *J. Am. Chem. Soc.*, 2011, **133**, 10629.
8 (*a*) T. Zhang, H. Fan, G. Liu, J. Jiang, J. Zhou and Q. Jin, *Chem. Commun.*, 2008, 5414; (*b*) O. S. Wolfbeis, A. Dü rkop, M. Wu and Z. Lin, *Angew. Chem., Int. Ed.*, 2002, **41**, 4495.
9 (*a*) H. M. Kim and B. R. Cho, *Acc. Chem. Res.*, 2009, **42**, 863; (*b*) F. Helmchen and W. Denk, *Nat. Methods*, 2005, **2**, 932; (*c*) J. M. Squirrell, D. L. Wokosin, J. G. White and B. D. Bavister, *Nat. Biotechnol.*, 1999, **17**, 763.
10 (*a*) W. R. Zipfel, R. M. Williams and W. W. Webb, *Nat. Biotechnol.*, 2003, **21**, 1369; (*b*) L. Li, X. Shen, Q. Xu and S. Q. Yao, *Angew. Chem., Int. Ed.*, 2013, **52**, 424; (*c*) H. Ahn, K. E. Fairfull-Smith, B. J. Morrow, V. Lussini, B. Kim, M. V. Bondar, S. E. Bottle and K. D. Belfield, *J. Am. Chem. Soc.*, 2012, **134**, 4721; (*d*) H. C. Heo, K. H. Kim, H. J. Kim, S. H. Baik, H. Song, Y. S. Kim, J. Lee, I. Mook-jung and H. M. Kim, *Chem. Commun.*, 2013, **49**, 1303; (*e*) Q. L. Xu, C. H. Heo, G. Kim, H. W. Lee, H. M. Kim and J. Yoon, *Angew. Chem., Int. Ed.*, 2015, **54**, 4890.
11 P. Li, W. Zhang, K. X. Li, X. Liu, H. B. Xiao, W. Zhang and B. Tang, *Anal. Chem.*, 2013, **85**, 9877.

12 (*a*) X. H. Dong, C. H. Heo, S. Y. Chen, H. M. Kim and Z. H. Liu, *Anal. Chem.*, 2014, **86**, 308; (*b*) H. B. Yu, Y. Xiao and L. J. Jin, *J. Am. Chem. Soc.*, 2012, **134**, 17486.

13 (*a*) C. Chung, D. Srikun, C. S. Lim, C. J. Chang and B. R. Cho, *Chem. Commun.*, 2011, **47**, 9618; (*b*) K. M. Zhang, W. Dou, P. X. Li, R. Shen, J. X. Ru, W. Liu, Y. M. Cui, C. Y. Chen, W. S. Liu and D. C. Bai, *Biosens. Bioelectron.*, 2015, **64**, 542; (*c*) H. C. Guo, H. Aleyasin, S. S. Howard, B. C. Dickinson, V. S. Lin, R. E. Haskew-Layton, C. Xu, Y. Chen and R. R. Ratan, *J. Biomed. Opt.*, 2013, **18**, 106002.

14 (*a*) G. Masanta, C. H. Heo, C. S. Lim, S. K. Bae, B. R. Cho and H. M. Kim, *Chem. Commun.*, 2012, **48**, 3518; (*b*) J. Jing and J. L. Zhang, *Chem. Sci.*, 2013, **4**, 2947.

15 (*a*) H. R. Petty, *Biochim. Biophys. Acta*, 1989, **1012**, 284; (*b*) P. Bellavite, *Free Radical Biol. Med.*, 1988, **4**, 225.

16 M. Y. Song, L. Z. Zeng, X. J. Hong, Z. H. Meng, J. F. Yin, H. L. Wang, Y. Liang and G. B. Jiang, *Environ. Sci. Technol.*, 2013, **47**, 2886–2891.

